A Three-D Circulation Model Study of the Radiative-Dynamic Coupling within the Stratosphere

V. Ramanathan[1])

George Washington University-NASA Langley Research Center

W. L. Grose

NASA Langley Research Center

Abstract: The objective of the present paper is to investigate the role of radiative transfer processes in the general circulation of the stratosphere. This objective is accomplished by comparing the thermal and dynamical structure of the stratosphere as simulated by two controlled numerical experiments. Both the experiments have been performed with the aid of a spectral 3-dimensional quasi-geostrophic circulation model. The only difference between the two experiments lies in the treatment of longwave radiative transfer within the stratosphere. In the first experiment, referred as Exp. 1 in the text, a detailed radiative transfer model is employed to treat the longwave radiative transfer in the stratosphere. In the second experiment, referred as Exp. 2 in the text, longwave radiative transfer is accounted for by employing the Newtonian cooling approximation.

The primary results obtained from the comparison study are given below: (i) The exchange of longwave radiation between the troposphere and lower stratosphere has a net heating effect on the lower stratosphere. It is shown that this heating effect contributes partly to the maintenance of the warm high-latitude belt in the lower stratosphere during winter and spring seasons. (ii) It is shown that the strong temperature dependence of the Newtonian cooling coefficient, h, plays an important role in determining the zonal temperatures as well as having a significant influence on the transmissivity of stratosphere to propagating planetary scale waves. (iii) It is shown that the temperature dependence of h is such that it facilitates the propagation of planetary scale waves in the stratosphere during winter and spring time.

1. Introduction

This paper describes the results of a numerical experiment that was designed to examine the role of radiative transfer processes in determining the thermal and dynamical structure of the stratosphere. The numerical experiment was performed with the aid of a three-dimensional circulation model developed by the authors at the NASA-Langley Research Center.

Several theoretical and observational studies (MANABE and HUNT 1968, OORT 1964 amongst many others – the reader is referred to HOLTON (1975) for a comprehensive bibliography on this subject) on the stratospheric general circulation have been reported in the literature. These studies indicate that, both the *in situ* solar heating by ozone and the dynamical forcing of the stratosphere by the troposphere play an important role in the general circulation of the statosphere. For example, during winter and spring seasons the latitudinal gradient of the tropopause and lower stratosphere temperatures are primarily caused by the mean and eddy motions orginating from the troposphere. Furthermore, bulk of the eddy kinetic and potential energy within the stratosphere owe their presence to the upward propagation of planetary scale waves from the troposphere.

[1]) Presently with the National Center for Atmospheric Research which is sponsored by the National Science Foundation. The analysis of the results presented herein were performed at NCAR.

In addition to the mechanisms discussed above, there are two other processes which have not been given sufficient attention in the previous publications. The first of these concerns the radiative coupling between the troposphere and the lower stratosphere. This coupling arises from the exchange of longwave radiative energy between the troposphere and the lower stratosphere. The troposphere is in general much warmer than the lower stratosphere and consequently has a heating effect on the lower stratosphere. Furthermore, the strong latitudinal gradient in the tropospheric temperatures would induce a latitudinal gradient in the heating of the tropopause and the lower stratosphere. It would be of interest to examine the effect of this radiative coupling on the dynamics of the lower stratosphere. The second process concerns the effect of stratospheric radiative transfer processes on the response of the stratosphere to propagating planetary waves. Longwave radiative cooling within the stratosphere dissipates planetary waves. This dissipation attenuates the waves and also leads to a nonzero divergence of the upward energy flux associated with the propagating planetary waves (DICKINSON, 1969). The radiative dissipation of the waves is proportional to the Newtonian cooling coefficient (i e., the inverse of the radiative time constant), h. The value of h increases with temperature. For example, at the 10 mb level, the value of h at a temperature, T = 280 °K, is larger by a factor of 2–3 than that at T = 220 K. Since T is a function of latitude, the temperature dependence of h implies that h is also a strong function of latitude. It then follows that there is a strong latitudinal gradient in the rate of radiative dissipation, either of propagating waves or dissipation of zonal and eddy available potential energy. The question that has not been considered in detail is: what effects do the latidudinal gradient in h have on the strapospheric circulation?

The primary objective of the present paper is to provide a better understanding of the importance of the two processes mentioned above to the general circulation of the stratosphere. Towards this goal the following two numerical experiments have been performed: (i) Experiment 1: In this experiment, a quasi-geostrophic circulation model (the details of this model are given later) is coupled with a detailed radiative transfer model described in RAMANATHAN (1976). (ii) Experiment 2: This experiment employs the same dynamical model used in Expt. 1. The longwave cooling within the stratosphere is calculated by the Newtonian cooling approximation. Furthermore, the Newtonian cooling coefficient is assumed to be only a function of altitude. It should be noted that the solar heating by O_3 and the radiation model used for the troposphere is identical in both experiments. Thus the only difference between the two experiments is in the treatment of longwave radiative transfer within the stratosphere. The state of the stratosphere [defined by global distribution of temperature, zonal winds, global values of available zonal and eddy potential energy and zonal and eddy kinetic energy] as simulated by the two experiments will be compared. The comparison study has been performed for model simulation of "steady state" solstice and equinox conditions and for model simulation of the complete seasonal cycle. In this study we will present results from the steady state runs while results from the seasonal cycle experiments will be published elsewhere.

As explained below, such a comparison study can be expected to accomplish the stated objectives of the present paper. The Newtonian cooling approximation assumes implicitly that the longwave cooling at any level in the atmosphere is solely proportional to the temperature at that level and consequently this approximation neglects the exchange of radiative energy between layers within the stratosphere. Hence, a comparison of the two experiments would indicate the importance of radiative coupling between the troposphere and lower stratosphere which arises due to the exchange of radiative energy between layers. Further, recall that in the experiment that employs the Newtonian cooling approximation, h has been assumed to be a function of only altitude and not temperature whereas the experiment that employs the detailed radiative transfer model accounts for all of the temperature dependency of h and hence this experiment accounts for the latitudinal gradient in h. Hence, a comparison of the two experiments would illustrate the importance of th latitudinal gradient in h to the stratospheric circulation. In addition, the comparison study will also serve another useful purpose. Some of the currently available stratospheric models employ the Newtonian cooling approximation and the present study would enable a better understanding of the limitation, if any, of such models for realistic stratospheric studies.

2. Model Description

The model developed for the study is a spectral quasi-geostrophic model. A combination of the procedures given in TRENBERTH (1973) and CUNNOLD *et al.* (1975) has been adopted for the treatment of dynamics. The model adopts the quasi-geostrophic system of equations in pressure, P, coordinates. The equations are derived in TRENBERTH and hence will not be given here. The system of equations contains one prognostic equation for the vertical component of the relative vorticity, ζ, and two diagnostic equations, namely the thermal wind equation and the ω-equation respectively for the potential temperature and ω which is the equivalent of the vertical velocity in the P-coordinate system. The model adopts finite differencing in the vertical direction, while the latitudinal and longitudinal dependence of the field variables are expressed in terms of truncated series of surface spherical harmonics. The truncation scheme is the same as that given in CUNNOLD *et al.* (1975) and in this scheme any variable, ζ, is expressed as

$$\zeta(\lambda, \mu, P, t) = \sum_{M=-6}^{+6} \sum_{N=N1}^{N2} \zeta_N^M(P, t)\, Y_N^M(\mu, \lambda) \qquad (1)$$

$$\begin{aligned} N1 &= 1 \text{ when } M = 0 \\ &= |M| \text{ when } M \neq 0 \\ N2 &= N1 + 5 \end{aligned} \qquad (2)$$

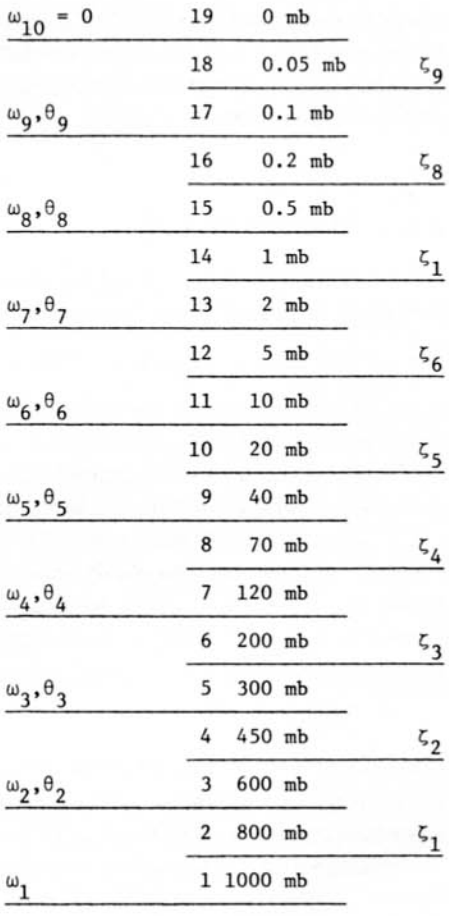

● **Figure 1**
Vertical resolution in the model. θ is the potential temperature. The variables ζ and ω are explained in the text.

where t, λ and μ are respectively the time, the longitude and the sine of latitude, ζ_N^M is the spectral coefficient which is a function of t and P and Y_N^M is the surface spherical harmonic whose properties are well documented in the literature (for example see PLATZMAN, 1962). In Eq. (1) M is the logitudinal wave number and N denotes the degree of the spherical harmonic. Components with negative M can be expressed as complex conjugate of the components with positive M such that, as seen from Eqs. (1) and (2), each variable in the model is expressed in terms of 42 spectral components at each pressure level. The nonlinear terms in the equations are computed in the spectral domain by the interaction coefficient method as explained in TRENBERTH (1973). For the integration of the model with respect to time, the N-cycle time differencing scheme of LORENZ (1971) is adopted and the fundamental time step in the model is 1 hour. The model adopts the 4-cycle version of LORENZ's N-cycle scheme.

The vertical resolution adopted in the model is shown in Figure 1 and is identical to TRENBERTH's model. The variables ω and θ are specified at odd levels and ζ is specified at even levels such that the model effectively has nine levels in the vertical. In the thermodynamic energy equation, the model assumes the static stability to be independent of longitude, latitude and time of the year, an assumption which is conventional in quasi-geostrophic models. The boundary conditions need to be specified only for ω and following TRENBERTH (1973) we let

$$\begin{aligned} \omega &= 0 \text{ at the top of the model atmosphere} \\ &= -\rho_0 g\, J(\psi, H) \text{ at } P = P_0 \end{aligned} \tag{3}$$

where ρ_0 and P_0 are respectively the density and pressure at the bottom boundary, g is the acceleration due to gravity and $J(\psi, H)$ is the Jacobian of the stream function, ψ, and the orography. The bottom boundary condition includes approximately the effects of orography. The specification of the height profile for the orography is identical to the one given in TRENBERTH.

2.1. Diabatic Heating

Within the troposphere, i.e. the region defined by $1000 \leqslant P < 120$ mb in the model, the diabatic heating, Q, is treated by the Newtonian cooling approximation given by,

$$Q = h(P)\,[\theta^*(P, \mu, \lambda, t) - \theta(P, \mu, \lambda, t)] \tag{4}$$

where θ^* is an equilibrium temperature and θ is the actual temperature. The values of h and θ^* are obtained from TRENBERTH (1973). It should be mentioned that the nonzonal heating effects due to the contrast between land and sea surface temperatures have been incorporated in the definition of θ^*. The formulation given by Eq. (4) is admittedly crude but the results shown in TRENBERTH (1973) and CUNNOLD *et al.* (1975) seem to indicate that it simulates reasonably well those features of the tropospheric circulation which are of importance to the dynamical forcing of the stratosphere.

Within the stratosphere, which, for the purposes of the present description is the region of the model defined by 120 mb $\leqslant P \leqslant 0$ (note that the 120 mb level is included as a part of the stratosphere), the source for diabatic heating is radiative heating and cooling. The Q for the stratosphere can be written as

$$Q = Q^S + Q^{LW}$$

where the Q^S and Q^{LW} denote respectively solar heating and longwave cooling.

For both the experiments mentioned earlier in the introduction, the solar heating is calculated by the procedure given in RAMANATHAN (1976) which includes the solar heating due to O_3, H_2O and CO_2. The mixing ratios of CO_2 and H_2O within the stratosphere are assumed to be 320 ppm (by volume) and 3 ppm (by mass) respectively. For O_3, the seasonal and latitudinal distributions given in DOPPLICK (1970)

■ **Table 1.** Global Ozone Mixing Ratio (μgm/gm)

	Latitude												
P	78	65	52	39	26	13	0	13	26	39	52	65	78
mb		Summer Solstice							Winter Solstice				
.1	.4	.4	.4	.4	.4	.4	.4	.4	.4	.4	.4	.4	.4
.5	1.7	1.7	1.7	1.7	1.7	1.7	1.7	1.7	1.7	1.7	1.7	1.7	1.7
2	6.5	7.1	7.7	7.9	7.6	8.2	8.4	8.6	9.0	10.1	10.6	8.6	5.3
10	7.7	8.6	10.0	11.7	12.8	13.5	14.1	13.6	11.4	9.9	9.1	8.3	7.8
40	5.2	5.1	5.2	5.2	4.9	4.6	4.6	5.1	6.2	7.3	7.3	6.9	6.6
120	1.8	1.5	1.1	.7	.48	.27	.17	.18	.47	1.1	1.9	2.5	2.8
300	.41	.37	.29	.19	.11	.07	.05	.05	.08	.18	.33	.37	.36
600	.07	.07	.08	.09	.07	.05	.05	.05	.06	.07	.07	.07	.07
1000	.05	.05	.05	.05	.05	.05	.05	.05	.05	.05	.05	.05	.05
P	78	65	52	39	26	13	0	13	26	39	52	65	78
mb		Fall Equinox							Spring Equinox				
.1	.4	.4	.4	.4	.4	.4	.4	.4	.4	.4	.4	.4	.4
.5	1.7	1.7	1.7	1.7	1.7	1.7	1.7	1.7	1.7	1.7	1.7	1.7	1.7
2	4.5	5.5	6.0	6.0	6.0	6.0	6.0	6.0	6.3	6.6	6.6	6.2	5.3
10	6.3	7.6	8.8	10.4	11.9	13.3	14.4	14.2	12.7	11.3	10.6	9.4	8.5
40	4.8	5.1	5.4	5.3	5.0	4.7	4.5	5.0	6.1	7.2	7.4	7.4	7.1
120	1.8	1.4	1.0	.6	.4	.2	.18	.3	.5	1.1	2.0	2.4	2.7
300	.27	.25	.17	.13	.08	.07	.06	.08	.1	.25	.35	.5	.7
600	.05	.05	.05	.07	.07	.06	.05	.06	.07	.09	.07	.07	.08
1000	.05	.05	.05	.05	.05	.05	.05	.05	.05	.05	.05	.05	.05

have been adopted. DOPPLICK gives O_3 distributions only up to 10 mb level. Due to lack of sufficient global data at the higher levels, a latitudinally independent mixing ratio is assumed at the 0.1 and 0.5 mb level and this mixing ratio value corresponds to globally averaged conditions. The mixing ratio values at the 2 mb level is obtained by interpolating the values at the 10 mb and 0.5 mb levels. The adopted global ozone distribution is shown in Table 1.

As mentioned earlier the method adopted for longwave cooling computations in the stratosphere is different for the two experiments. For Expt. 1 the detailed radiative transfer model described in RAMANATHAN (1976) is adopted. This model includes longwave cooling due to H_2O, O_3 and CO_2. The model also includes Doppler broadening effects and several hot bands of CO_2. The mixing ratio of O_3 is given in Table 1 and for H_2O, a fixed relative humidity distribution as given by MANABE and WETHERALD (1967) is adopted. The model also accounts for clouds as described in RAMANATHAN (1976).

For Expt. 2 longwave cooling is computed by the approximate method involving the Newtonian cooling approximation, i.e. by letting

$$Q^{1W} = \langle Q(P) \rangle + h[\bar{T}(P) - T(P, \lambda, \mu, t)] \tag{6}$$

where $\bar{T}(P)$ is the globally averaged temperature and $\langle Q(P) \rangle$ is the globally averaged longwave cooling. Since in the present model $\bar{T}(P)$ is prescribed, $\langle Q(P) \rangle$ need not be evaluated and hence we will omit any further reference to this term. The values for h are obtained from TRENBERTH (1973). As mentioned earlier h is a function of only the vertical coordinate.

2.2. Time Integration Scheme

The model was initiated from a state of rest. At this stage, only the zonal heating was prescribed and the zenith angle of the sun was fixed at equinoctial conditions. After integrating the model for a period of three months the nonzonal heating and the orography effects were included and the model was integrated for an additional period of six months. Due to the wave-wave interaction all of the spectral components were activated. The result obtained from the last 30 days of this run is referred to as "steady state" equinox simulation in the text. The seasonal heating cycle was started at this stage and the model was integrated for a period of thirly months. The simulation of the last twelve months is taken for the seasonal cycle experiments. The last day of the seasonal cycle corresponds to the solstice conditions (winter solstice in the northern hemisphere). The steady state solstice simulation was obtained by taking the last day's simulation of the seasonal cycle experiment as the initial condition and integrating the model for 90 days with the sun fixed at the solstice. The results obtained from the last 30 days of this run is taken as the steady state solstice simulation. The procedure described above is adopted for both the experiments.

3. Model Validation

As mentioned earlier the time integrations have been performed to simulate the yearly seasonal cycle and steady state solstice and equinox conditions. In this section, we will compare the model results for the stratospheric climate, as obtained from the seasonal cycle simulation of Expt. 1, with observed values and with the previous model study of MANABE and HUNT (1968).

The mean monthly zonal winds and temperatures simulated by the model for January, i.e. the northern hemisphere winter and southern hemisphere summer, are shown respectively in Figures 2 and 3. It is seen from Figure 2 that the model simulates the altitude and latitude location of the tropospheric jet in both the summer and winter hemispheres. However the intensity of the winter hemispheric jet is much smaller

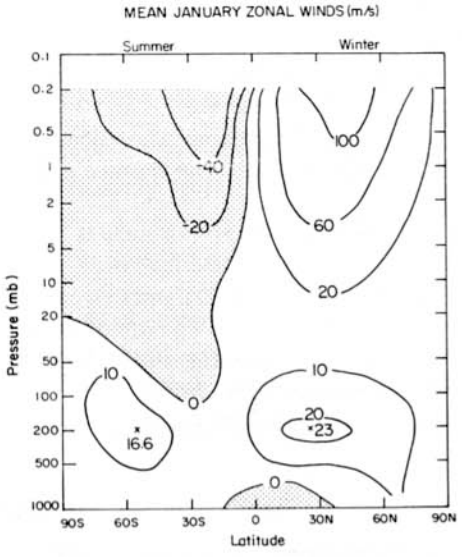

- **Figure 2**

The mean zonal winds for January obtained from the annual cycle for Expt. 1. Units: $m \cdot S^{-1}$.

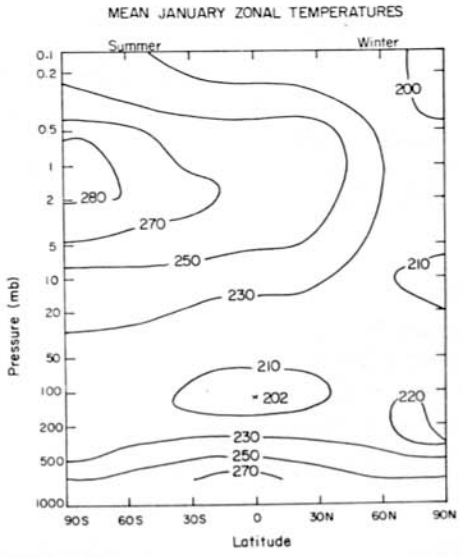

- **Figure 3**

Mean zonal temperatures for January obtained from the annual cycle for Expt. 1.

than the observed value of 30–35 m · S^{-1} (NEWELL *et al.*, 1970). Surface easterlies in the low latitudes are also simulated. But the observed extension of the stratospheric easterlies in the low latitude troposphere is not simulated. This deficiency exists in the previous quasi-geostrophic models also (see CUNNOLD *et al.*'s results). Further within the stratosphere the model reproduces the easterlies in the summer hemisphere and westerlies in the winter hemisphere. The model also simulates the poleward tilt of the axis of the maximum zonal wind in the winter hemisphere. The magnitude of the wind in the region between 100 mb and 5 mb is in good agreement with the observed values of NEWELL *et al.* (1970) and LEOVY and WEBSTER (1976). Above this region, the maximum zonal wind predicted by the model is much larger than the observed value of NEWELL but is in good agreement with LEOVY and WEBSTER's value. For example at the 0.5 mb level, the model predicts a maximum wind 100 m · S^{-1} while NEWELL's value is 80 m · S^{-1} and LEOVY and WEBSTER's value is 110 m · S^{-1}. These two observed values probably reflect the natural variability of the zonal winds caused by the presence (or absence) of events that lead to a break down of the winter polar vortex and subsequently resulting in "sudden" stratospheric warming (HOLTON, 1975).

The zonal temperatures shown in Figure 3, indicate that the model simulates the overall features of the atmosphere up to about 1 mb while above this region the model is deficient in simulating even the qualitative features of the observed temperature profile. The model simulates the cold equatorial tropopause temperature and the poleward increase in temperature in both the hemispheres within the lower stratosphere. The model clearly shows that the maximum temperature within the stratosphere occurs at the 1–2 mb level in the summer polar regions, a feature which is observed in the actual stratosphere. However in the region above 0.2 mb the model does not reproduce the observed maximum temperatures in the winter polar regions. As discussed by CUNNOLD *et al.* (1975) this deficiency may be caused by the upper boundary conditions.

It is also of interest to compare the present model with MANABE and HUNT's (1968) model to indicate the validity of quasi-geostrophic formulation for stratospheric studies. For this purpose we compare the transport of heat by the dynamical processes. It should be cautioned at this stage that MANABE and HUNT's model includes the transport of heat by large-scale eddies, mean meridional motion and small-scale convection while the present model includes only the former two processes. Further with respect to heat transport by mean meridional motions, MANABE and HUNT's model includes the transport of heat by both the vertical and latitudinal motions while the present model includes only the transport of heat by vertical motions. However, it is seen from MANABE and HUNT's results that the contribution by small-scale convection and mean latitudinal motions to the transport of heat is negligible above 120 mb and hence it seems appropriate to compare the two models.

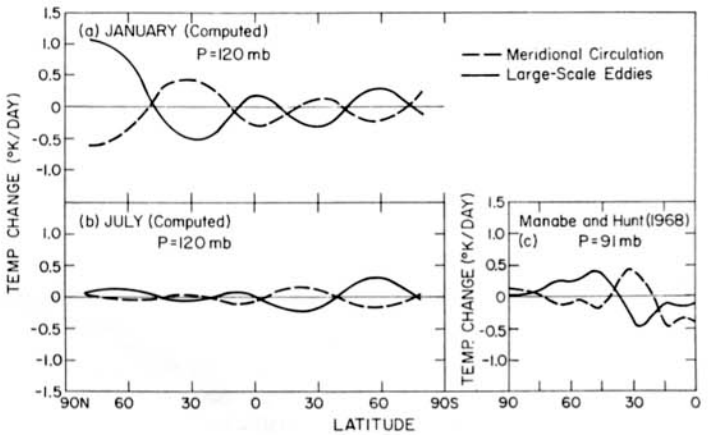

Figure 4

Comparison of the dynamical heat balance components for the lower stratosphere.

The heating rates computed by the present model for January and July conditions are compared with MANABE and HUNT's results in Figures 4–6. An exact comparison is not possible for the following reasons: (1) MANABE and HUNT's model is a hemispherical model while the present model is a global model. (2) MANABE and HUNT's results are for annual mean conditions. Since MANABE and HUNT state that their model simulation reflects winter conditions, we have shown the present model results for January (NH winter) and for July (SH winter) conditions.

Consider first the 120 mb level heating rates shown in Figure 4. It is seen that the two models agree qualitatively in that both the models predict heating by eddies north of about 50° and cooling in the low latitudes. Further, the cooling in the equatorial and subtropical latitudes, warming in midlatitudes and cooling in high latitudes by the meridional circulation is similar in both the models. However, the exact location of the latitude of the alternate cooling and warming effects are appreciably different in the two models. Now, considering the 10 mb and 2 mb cooling rates, it is seen that both the models are similar in that they show the increase in the magnitude of the respective heating (or cooling) rates with altitude. Further it is seen that, at high latitudes, both the models indicate the almost exact cancellation of the heating and cooling rates between the eddy and mean meridional term.

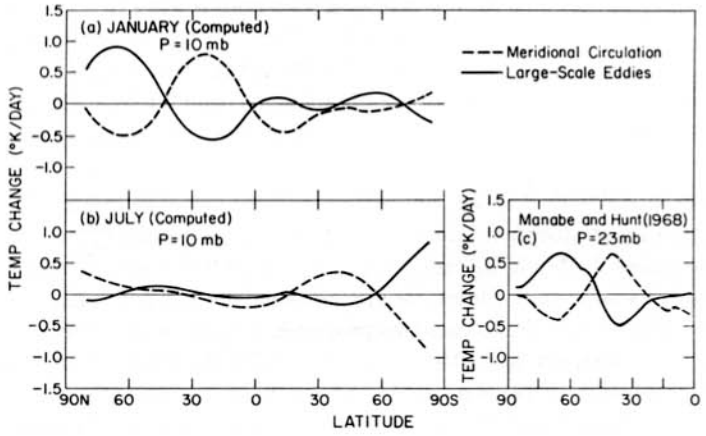

Figure 5
Comparison of the dynamical heat balance components for the middle stratosphere.

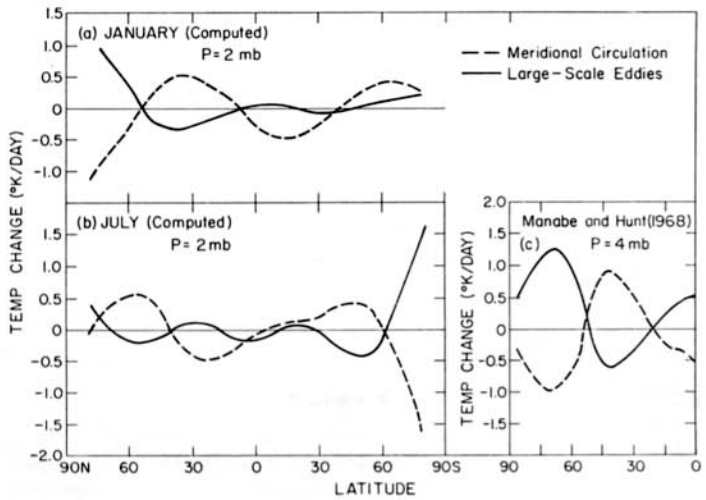

Figure 6
Comparison of the dynamical heat balance components for the upper stratosphere.

The seasonal and latitudinal dependency of the heating rates at the 120 mb level (Figure 4) reveal the following interesting features. The January and July profiles indicate that the eddy heating is much larger in the winter hemisphere than in the summer hemisphere. This is due to the fact the eddy activity in the troposphere is much larger in the winter hemisphere. Further, upon comparing the respective winter hemispheres (i.e., the northern hemisphere in January and the southern hemisphere in July) it is seen that the heating terms are much larger in the northern hemisphere. The imposed orography profile and the nonzonal heating terms are much larger (by a factor of 2 or more) in the northern hemisphere and consequently the eddy heating terms are much larger in the northern hemisphere winter.

4. Results of the Comparison Study

It is seen that there are systematic differences between the two experiments in the predicted zonal temperatures, zonal winds and the energy components (i.e., zonal and eddy potential energy and kinetic energy). A detailed description of these results is given here. The results have also been analyzed in detail to explain the sources for the differences. The results of this analysis for the zonal temperatures and winds are given here while the analysis of the energetics will be published elsewhere.

For the purposes of the present description temperature will be denoted by T, the zonal wind by $\bar{U}$ and further $T(1)$ and $\bar{U}(1)$ will denote the values of T and $\bar{U}$ for Expt. 1 while $T(2)$ and $\bar{U}(2)$ will denote the respective values for Expt. 2. Recall that Expt. 1 employs the detailed radiative transfer model in the stratosphere while Expt. 2 employs the Newtonian cooling approximation. As mentioned earlier, we will present results of the comparison study for the steady state solstice and equinox conditions.

4.1. The Zonal Temperatures

The qualitative and quantitative nature of the differences between the two experiments are similar for both the solstice and equinox simulations and hence we will present figures only for the solstice simulation.

(a) *Lower stratospheric temperatures (120 mb and 40 mb levels):* For the purpose of this model, the 120 mb level can be considered as the tropopause. The altitude of this level is 15 km which is the approximate location of the equatorial tropopause. Further the model predicts the minimum temperatures at this level and consequently this level can be termed as the tropopause for the model. The results for the 120 mb level are shown in Figures 7(a), 7(b), and 7(c). As seen from 7(b), Expt. 2 overestimates T at the high latitudes and slightly underestimates T at the midlatitudes. From 7(a) and 7(b) it is seen that Expt. 1 simulates the warm belt in winter at around 60 ° N while Expt. 2 predicts, unrealistically, the temperature to increase monotonically from equator to pole in the winter [as can be seen by subtracting the values given in 7(b) from 7(a)]. The sources for these differences can be explained by considering Figures 7(c). Figure 7(c) shows the various heat balance components as obtained from Exp. 1. In 7(c) Q^S is the solar heating and Q^{Ex} is the net longwave heating at the 120 mb level due to exchange of longwave energy between the 120 mb level and the troposphere and surface. The dynamical heating term includes both the eddy and mean meridional heating terms. In Expt. 2 the longwave cooling is computed by the Newtonian cooling approximation and hence Q^{Ex} term is completely neglected. This is one of the primary differences between the two experiments and it is argued below that the differences in T's between the two experiments can be explained based on the neglect of Q^{Ex} in Expt. 2. It is seen from 7(c) that Q^{Ex} is maximum in the region between 30 and 45° and Q^{Ex} decreases poleward from 45°. The tropospheric temperature decreases poleward and consequently Q^{Ex} decreases poleward. The maximum in Q^{Ex} between 30° and 45° is due to the 9.6 μm band O_3 heating. The forcing term in the quasi-geostrophic model is the

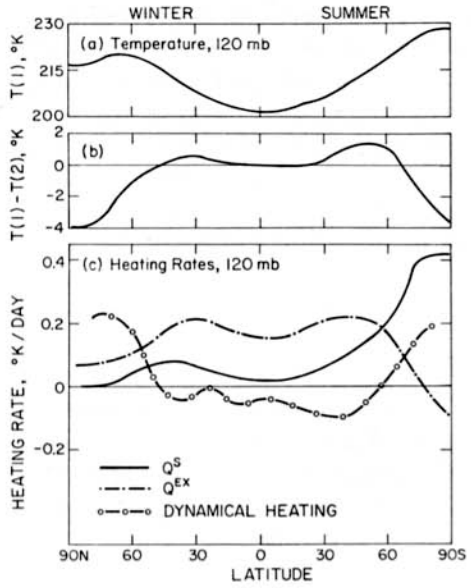

● **Figure 7**

Comparison of the 120 mb zonal temperatures for solstice. The heating rates shown in (c) are obtained from Expt. 1. Q^S is the solar heating and Q^{Ex} is the heating (or cooling) by exchange of longwave radiation.

departure from the global average. As can be deduced from 7(c) the departure of Q^{Ex} from the globally averaged value is positive in the low latitude and will be negative in the high latitude. Since Expt. 2 neglects the Q^{Ex}, it follows from the preceding arguments that $T(1) > T(2)$ in low latitudes and $T(1) < T(2)$ in high latitudes.

It can also be concluded from Figure 7 and from the previous discussions that the rapid decrease of Q^{Ex} at the high latitudes contributes partly to the decrease in winter temperatures from 60° to the pole. Thus, we are led to the conclusion that the differential longwave heating effect of the troposphere on the tropopause plays a nonnegligible role in maintaining the warm belt at 60° latitude during winter and spring. This is an important result and its significance can be appreciated by noting that the previous quasi-geostrophic models (TRENBERTH, 1973; CUNNOLD *et al.*, 1975 and others) have not been able to simulate the high latitude warm belt at the tropopuase level. It should be noted that, by a striking coincidence all of these models employ the Newtonian cooling approximation which as we have pointed out neglects the latitudinal variation of Q^{Ex}.

The difference in the latitudinal profile of the 40 mb temperatures between the two experiments is similar to the difference in the 120 mb temperatures. Again, most of the differences in the 40 mb temperatures is due to the neglect of the Q^{Ex} term in Expt. 2.

(b) *The middle stratospheric temperatures [10 mb level]:* The results of the comparison study for the 10 mb level are shown in Figures 8(a)– (d). Figure 8(a) also shows the assumed value of $\langle\overline{T}\rangle$ where $\langle\overline{T}\rangle$ is the horizontally averaged value of T at the 10 mb level. The observed value of T are taken from LABITZKE (1972). In order to explain the differences shown in 8(b), we have to consider both the Q^{Ex} term shown in 8(c) and the latitudinal dependence of h shown in 8(d). It is seen that Q^{Ex} is positive in the winter high latitude regions while it is negative in the summer hemisphere. This is because in the winter high latitude regions the temperature decreases with altitude up to 2 mb and consequently the 10 mb level is being warmed radiatively by the lower levels. Just the reverse situation exists in the summer hemisphere. This effect of Q^{Ex} is not included in Expt. 2 and consequently the latitudinal variation in Q^{Ex} would partly explain the larger value of T(1) at the winter polar regions and smaller value of T(1) in the summer hemisphere. However, there is yet another major difference between the two experiments and this concerns

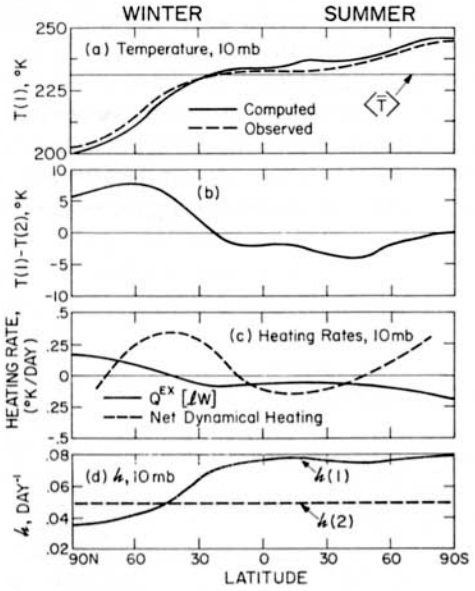

● **Figure 8**

Comparison of the 10 mb zonal temperatures and h. h is the Newtonian cooling coefficient. $\langle \bar{T} \rangle$ is the assumed globally averaged temperature.

the temperature dependence of h. The values of h(1) and h(2) are shown in Figure 8(d). It should be noted that Expt. 1 does not employ the Newtonian cooling approximation. However for comparison purposes, the value of h(1) was computed from the radiative transfer model used in Expt. 1 by adopting the temperature distribution computed by Expt. 1. It is seen from 8(d) that h(1) has a strong latitudinal variation, the reason being: h is a strong function of temperature and since T is a strong function of latitude h is a strong function of latitude, as opposed to Expt. 2 in which h is independent of latitude. We will examine the effect of the differences in h on T. Consider the energy equation given by

$$\frac{\partial T}{\partial t} = (F_D + Q^s) - h(T - \langle \bar{T} \rangle) \tag{7}$$

where F_D is the dynamical heating and the other symbols in Eg. (7) have previously been explained. For strictly steady state conditions the left-hand side vanishes. As mentioned earlier Q^s is the same for both the experiments. For the purposes of the present arguments, we will assume that F_D is the same for both the experiments. It can then be easily shown that

$$\begin{aligned} &| T(1) - \langle \bar{T} \rangle | < | T(2) - \langle \bar{T} \rangle | \text{ when } h(1) > h(2) \\ &| T(1) - \langle \bar{T} \rangle | > | T(2) - \langle \bar{T} \rangle | \text{ when } h(1) < h(2) \end{aligned} \tag{8}$$

From Eq. (8) the following relations hold when $T > \langle \bar{T} \rangle$

$$T(1) - T(2) \left\{ \begin{array}{l} < 0 \text{ when } h(1) > h(2) \\ > 0 \text{ when } h(1) < h(2) \end{array} \right. \tag{9}$$

and when $T < \langle \bar{T} \rangle$

$$T(1) - T(2) \left\{ \begin{array}{l} > 0 \text{ when } h(1) > h(2) \\ < 0 \text{ when } h(1) < h(2) \end{array} \right. \tag{10}$$

The trend of the T(1) − T(2) curve in Figure 8(b) can easily be explained based on Eqs. (9) and (10). For example, consider 8(a) from which it is seen that, between 30 ° N and 90 ° S $T > \langle \bar{T} \rangle$ and from 8(d) it is

seen that $h(1) > h(2)$ for the region between 30 °N and 90 °S and for these conditions it follows from Eq. (9) that $T(1) - T(2) < 0$ as indeed shown in Figure 8(b). Finally consider the region 60 °N to 90 °N. In this region $T(1) < \langle \bar{T} \rangle$ and $h(1) < h(2)$ [see Figures 8(a) and (d)]. From Eq. (10), for these conditions $T(1) - T(2) < 0$ but Figure 8(b) shows that $T(1) - T(2) > 0$. This discrepancy can be resolved by considering the Q^{Ex} term which, as explained earlier, tends to warm the high latitude regions in the winter. Since this warming effect is not included in Expt. 2, $T(1) > T(2)$. It follows that at the 10 mb level the temperature dependence of h plays a dominant role and the Q^{Ex} term plays a marginal role in determining the thermal structure of the stratosphere.

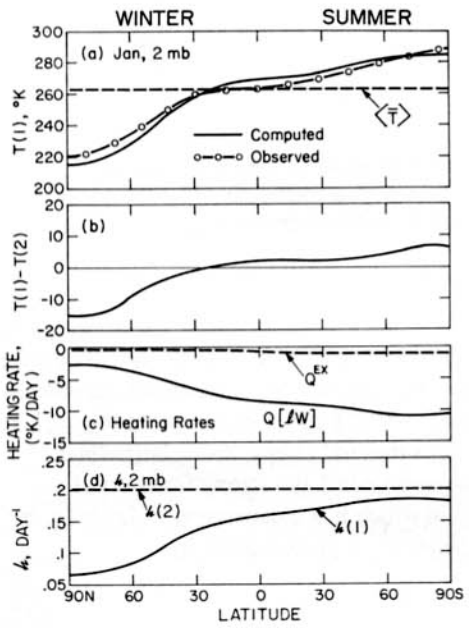

● **Figure 9**
Comparison of the 2 mb zonal temperatures and h.

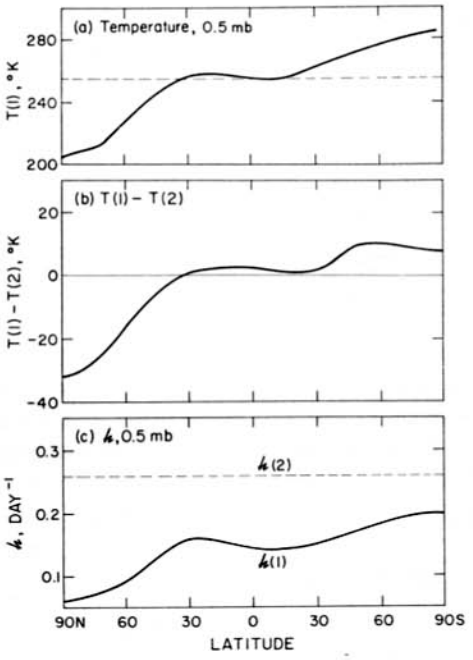

● **Figure 10**
Comparison of the 0.5 mb zonal temperatures and h.

(c) *The upper stratospheric temperatures (2 mb and 0.5 mb levels):* The results for these two levels are shown in Figures 9 and 10. The observed values of T are taken from LABITZKE (1972). In Figure 9(c) Q[1W] is the total longwave cooling and it is seen that the Q^{Ex} term is very small when compared with Q[1W], Hence, the main difference between the two experiments can be traced to the temperature dependence of h in Expt. 1.

The trend of the $T(1) - T(2)$ curves in Figures 9(b) and 10(b) can easily be explained by considering Figures 9(a), (c) and (d) and 10(a), (c) and (d) in conjunction with Eqs. (9) and (10). We will not be elaborating further since the trends are self-explanatory. It should be noted from Figures 9(b), 10(b), 9(d) and 10(d) that the absolute magnitude of $T(1) - T(2)$ is larger when the difference in h is larger.

It is appropriate at this stage to add the following note of caution regarding our interpretation of results. In interpreting the differences between the two experiments we have neglected to account for any differences in the dynamical processes between the two experiments. This is undoubtedly an oversimplication.

It is possible that differences between the two experiments in the dynamics may have contributed to the differences in the temperatures. Nevertheless, we express confidence in our interpretation for the following reasons: (1) The primary difference between the two experiments is in the treatment of longwave radiative transfer and any difference in the dynamics between the two experiments should be that caused by the differences in the radiation models. Hence, it seems reasonable to assume that the contribution to T(1) − T(2) arising from the changes in dynamics will be smaller than that arising from the direct effects of longwave radiative transfer. (2) Lastly, our interpretations explain the trend of T(1) − T(2) for the steady state simulations as well as the trend of T(1) − T(2) for the seasonal simulations (which have not been reported here) and hence the analysis can be considered statistically significant.

4.2 Comparison Study: Dynamical Aspects

In this section we will compare the zonal winds and the energy components between the two experiments.

The zonal winds obtained from the two experiments are compared in Figures 11(a) to (d). Most of the differences can be explained easily by considering the previously presented differences in the zonal temperatures in conjunction with the thermal wind equation.

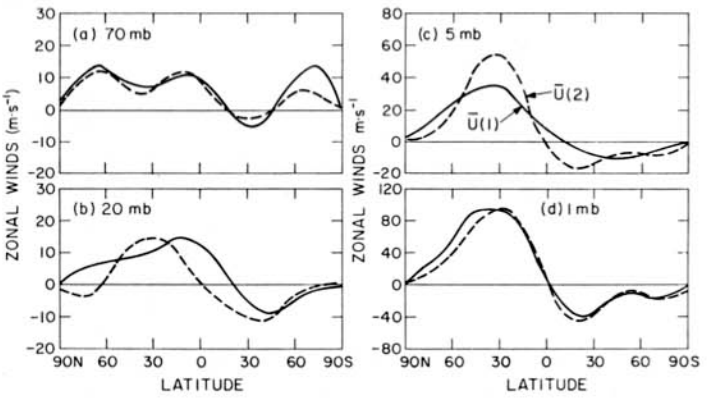

● **Figure 11**
Comparison of the zonal winds for the solstice. $\bar{U}$ (1) is the solid line and $\bar{U}$ (2) is the dashed line. Units: $m \cdot S^{-1}$.

Consider next the energy components within the stratosphere. The ratios of the available zonal and eddy potential energy (APZ and APE) and zonal and eddy kinetic energy (KZ and KE) between the two experiments are given in Table 2. The values of the four components are global values and not hemispherical values. The ratios of the four components are shown separately for the three regions of the stratosphere and for both the equinox and solstice simulations.

It is clearly seen from Table 2 that there are substantial differences between the two experiments in both the zonal and eddy components. The ratios of the zonal components can readily be explained based on the previous discussions on zonal temperatures and hence the present discussions will be focused on the eddy components. It is seen from Table 2 that, in all regions of the stratosphere, the eddy components are much larger in Expt. 1. The APE and KE computed by Expt. 1 is larger for both the equinox and solstice simulations and this fact attests to the statistical significance of the results. A qualitative explanation is given to explain the ratios of APE and KE shown in Table 2.

■ **Table 2.** Ratio of APE, KZ and KE between the two experiments. The Values of APZ, APE, KZ and KE are Global Values

	Equinox Stratosphere			Solstice Stratosphere			Comments
	Lower	Middle	Upper	Lower	Middle	Upper	
$\frac{APZ(1)}{APZ(2)}$	0.7	0.5	3.5	0.84	0.77	4.27	For APZ and APE: Lower = 200 – 20 MB Middle = 20 – 1 MB
$\frac{APE(1)}{APE(2)}$	1.1	1.5	5.0	1.06	1.35	2.23	Upper = 1 – .05 MB
$\frac{KZ(1)}{KZ(2)}$	1.3	0.9	1.2	0.93	0.79	1.43	For KZ and KE: Lower = 120 – 10 MB Middle = 10 – 0.5 MB
$\frac{KE(1)}{KE(2)}$	1.4	1.5	3.3	1.13	1.35	1.97	Upper = 0.5 – 0 MB

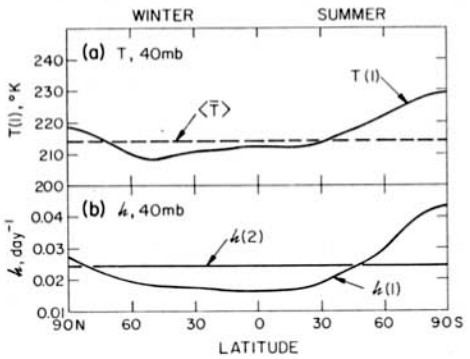

● **Figure 12**
(a) 40 mb zonal temperature for Expt. 1. (b) Comparison of h.

It is clear from MANABE and HUNT's (1968) study and DOPPLICK's (1970) study that most of the contribution to eddy energy within the stratosphere arises from planetary waves (primarily wave nos. 1, 2 and 3) propagating from the troposphere. From the studies of CHARNEY and DRAZIN (1961) and DICKINSON (1968 and 1969), the following conclusions concerning the transmissivity of the stratosphere to propagating waves can be arrived at: (1) the transmissivity, t, is almost zero in the presence of easterlies. (2) Even in the presence of westerlies, it is seen that there are minimum and maximum cutoff velocities below and above which t = 0. (3) the waves are dissipated by radiative processes. Based on the above three properties it is possible to explain qualitatively the differences in APE and KE between the two experiments. Due to property number (i), propagation of waves occurs mainly in the winter and spring hemisphere. Due to the presence of easterlies in the summer and fall hemisphere the transmissivity is negligible in these hemispheres. Further in the winter and spring hemispheres the stratospheric temperatures are such that $T << \langle \bar{T} \rangle$, particularly in the high latitudes (see Figures 8, 9 and 10). When $T << \langle \bar{T} \rangle$ it is seen from Figures 8, 9, 10 and 12 that $h(1) << h(2)$. Consequently, dissipation of waves is less in the winter and spring hemisphere in Expt. 1 as opposed to Expt. 2 in which h and hence the rate of dissipation is independent of seasons and latitudes. Summarizing the arguments, the combination of the following two factors contribute to the larger values of KE and PE in Expt. 1: (1) waves propagate mainly in the winter and spring hemisphere and (2) due to the temperature dependency of h(1), the

attenuation of waves is much less in the winter and spring hemispheres in Expt. 1. It is also possible that the differences in the energy components between the two experiments could have been caused by the differences in the dynamics. However, the mechanisms suggested here seem to be more important in causing the differences shown in Table 2. A more detailed analysis of the results have been performed by CHEN and RAMANATHAN (1977) and this analysis supports the qualitative explanations given here.

5. Concluding Remarks

The present paper reports a general circulation model experiment aimed at studying the relative role of dynamical and radiative processes within the stratosphere. The following are the principal conclusions.

(a) Longwave radiative transfer contributes in one of two ways to the thermal structure: (1) the heating by exchange of radiation between layers, Q^{Ex}; (2) the cooling to space. It is shown that Q^{Ex} plays an appreciable role in the lower stratosphere (i.e., $120 \leqslant P \leqslant 10$ mb) and Q^{Ex} is negligible above 10 mb. In the upper stratosphere ($P < 10$ mb) it is seen that the Newtonian cooling coefficient, h, is a strong function of temperature. This property of h plays an important role in determining the zonal temperatures as well as influencing significantly the transmissivity of stratosphere to propagating planetary scale waves.

(b) The results also reveal an important aspect of the propagation of waves in the stratosphere. Previous analyses (DICKINSON, 1968 and 1969) have shown that the stratospheric westerlies in the spring and winter hemispheres facilitate the propagation of planetary waves. The present analysis indicates the existence of another property of the winter and springtime stratosphere which also facilitates the propagation of planetary waves. It is shown that, during the winter and springtimes, due to the low stratospheric temperatures the value of h is small and consequently the radiative dissipation of planetyry waves is much smaller than the dissipation during summertime. Thus, the temperature dependence of h in conjunction with the low temperatures inreases the transmissivity of the stratosphere to propagating planetary waves during winter and spring seasons.

(c) Finally the results indicate that appreciable differences exist between a circulation model that incorporates the Newtonian cooling approximation and a model that incorporates a detailed radiative transfer model.

Acknowledgements

The authors would like to acknowledge the enthusiastic support of Mr. L. B. Callis, NASA-Langley Research Center, and the stimulating conversations with Dr. T.C. Chen. The analysis of the results presented herein and the preparation of this manuscript were done at the National Center for Atmospheric Research. The authors would like to thank Ms. Eileen Boettner of NCAR for typing the manuscript on short notice. Thanks are also due to the NCAR graphics department for the reparation of the figures.

References

CHARNEY, J.G., and P.G. DRAZIN, 1961: Propagation of planetary-scale disturbances from the lower into the upper atmosphere, J. Geophysical Research, 66, 83–109.

CHEN, T.C., and V. RAMANATHAN, 1977: In preparation.

CUNNOLD, D., F. ALYEA, N. PHILLIPS and R. PRIN, 1975: A three-dimensional dynamical-chemical model of atmospheric ozone, J. Atmospheric Sciences, 32, 170–194.

DOPPLICK, T,:1970: Global radiative heating with application to the dynamics of the lower stratosphere, Ph. D. Thesis, Massachusetts Institute of Technology.

DICKINSON, R,E., 1968: Planetary Rossby waves propagating vertically through weak westerly wind wave guides, J. Atmospheric Sciences, 25, 984–1002.

DICKINSON, R.E., 1969: Vertical propagation of planetyry Rossby waves through an atmosphere with Newtonian cooling, J. Geophysical Research, 74, 929–938.

HOLTON, J.R., 1975: The dynamic meteorology of the stratosphere and mesosphere, Meteorological Monographs, 15, No. 37.

LABITZKE, K., 1972: Climatology of the stratosphere in the northern hemisphere, Meteorologische Abhandlungen, Band 100/Heft 4, 1972.

LEOVY, C.B., and P.J. WEBSTER; 1976: Stratospheric longwaves: Comparison of thermal structure in the northern and southern hemispheres, J. Atmospheric Sciences, 33, 1624–1638.

LORENZ, E., 1971: An N-cycle time-differencing scheme for stepwise numerical integration, Monthly Weather Review, 99, 644–648.

MANABE, S., and R.T. WETHERALD, 1967: Thermal equilibrium of the atmosphere with a given distribution of relative humidity, J. Atmospheric Science, 24, 241–259.

MANABE, S., and B.G. HUNT, 1968: Experiments with a stratospheric general circulation model: 1. Radiative and dynamical aspects, Monthly Weather Review, 96, 477–502.

NEWELL, R., D. VINCENT, T. DOPPLICK, D. FERRUZZA and J. KIDSON, 1970: The Energy balance of the global atmosphere, The Global Circulation of the Atmosphere, G.A. Corby, ed., Royal Meteorological Society, 42–90.

OORT, A.H., 1964: On the energetics of the mean and eddy circulations in the lower stratosphere, Tellus, 16, 309–927, 1964.

PLATZMAN, G.W., 1962: The analytical dynamics of the spectral vorticity equation. J. Atmospheric Sciences, 19, 313–328.

RAMANATHAN, V., 1976: Radiative transfer within the earth's troposphere and stratosphere: A simplified radiative-convective model, J. Atmospheric Sciences, 33, 1330–1346.

TRENBERTH, K, 1973: Global model of the general circulation of the atmosphere below 75 kilometers with an annual heating, Monthly Weather Review, 101, 287–305.